Hindawi
Adsorption Science & Technology
Volume 2023, Article ID 2813663, 14 pages
https://doi.org/10.1155/2023/2813663

Research Article

Adsorptive Dephenolization of Aqueous Solutions Using Thermally Modified Corn Cob: Mechanisms, Point of Zero Charge, and Isosteric Heat Studies

Ositadinma Chamberlain Iheanacho,[1] **Joseph Tagbo Nwabanne**,[1] **Christopher Chiedozie Obi**,[2] **Chinenye Adaobi Igwegbe**,[1,3] **Chijioke Elijah Onu**,[1] **and Irvan Dahlan**[4]

[1]*Department of Chemical Engineering, Nnamdi Azikiwe University, P.M.B. 5025, Awka 420218, Nigeria*
[2]*Department of Polymer Engineering, Nnamdi Azikiwe University, P.M.B. 5025, Awka 420218, Nigeria*
[3]*Department of Applied Bioeconomy, Wroclaw University of Environmental and Life Sciences, Poland*
[4]*School of Chemical Engineering, Universiti Sains Malaysia, Engineering Campus, 14300 Nibong Tebal, Pulau Pinang, Malaysia*

Correspondence should be addressed to Christopher Chiedozie Obi; oc.christopher@unizik.edu.ng and Chinenye Adaobi Igwegbe; ca.igwegbe@unizik.edu.ng

Received 3 August 2022; Revised 18 October 2022; Accepted 27 March 2023; Published 13 April 2023

Academic Editor: Sami-ullah Rather

The sorption mechanisms, point of zero charge, and isosteric heats involved in the adsorptive dephenolization of aqueous solutions using thermally modified corn cob (TMCC) were studied at different initial phenol concentrations (100–500 mg/l), TMCC dosage (0.4–2.0 g), contact time (5–60 min), pH (2–10), and temperature (30–60°C). Analysis of the adsorbent material showed that it possessed the properties typical of a good adsorbent. The adsorption experiments revealed that phenol uptake is favored by an increase in TMCC dosage and contact time and a decrease in temperature and concentration of phenol in the solution. The experimental data were well-fitted to the Sips, Langmuir, Toth, and Redlich–Peterson isotherm models. Thermodynamic studies suggested that the sorption of phenol onto TMCC is feasible, spontaneous, and endothermic. The isosteric heats of adsorption obtained are in the range 47.43-79.38 kJ/mol, confirming that the adsorption process is predominantly a physical process depicting the van der Waals interactions, and it is inversely proportional to surface loading. The analysis of the adsorption mechanisms showed that the intraparticle, film, and pore diffusion mechanisms were significantly involved in the phenol adsorption process. The involvement of electrostatic attraction, π-π electron-donor interaction, and hydrogen bonding was also demonstrated. The point of zero charge (pH_{pzc}) was obtained at a pH of 5.83; being slightly lower than the optimum pH of 6 indicates that the sorbent surface is obviously not negatively charged at pH_{pzc}. The discoveries of this study have shown that the dephenolization process is feasible, spontaneous, endothermic, dominated by a physical process, and governed by intraparticle, film, and pore diffusion mechanisms.

1. Introduction

The release of phenol-contaminated effluents into aquatic environments calls for serious environmental concern. Phenols are very soluble in water; therefore, they can easily contaminate potable water of natural sources when they come in contact with them, thereby posing a danger to human health. The noxious effects of drinking phenol-contaminated water include sore throat, difficulty in swallowing, fainting, vomiting, headache, and liver and kidney damage as well as other mental illnesses [1–3]. The range of toxicity for both aquatic organisms and humans has been reported as 9-25 mg/l [4, 5]. Thus, the removal of phenols from phenol-contaminated effluents is statutorily obligatory so that their residual concentrations pose no serious environmental threat [6].

The most adapted technique for the decontamination of phenol-contaminated aqueous solutions is adsorption [7–12]. Lower design, development, and operating costs, operating ease, and high pollutant elimination efficiency are top of the reasons for the preference of adsorption over other alternative processes [1, 13–16]. The most widely used adsorbent for the removal of pollutants from wastewater is activated carbon (AC), mostly owing to its strong affinity for wastewater contaminants essentially because of its microporous structure, large surface area, enhanced surface reactivity, etc. [2]. However, the high cost of commercial AC made it obligatory for tailored research on the production of AC from renewable sources such as agro-waste products. Some of the agro-waste products that have been considered for the removal of phenol from aqueous solutions include palm kernel shell [17], onion dry scales [18], rice husk [19], wheat bran [20], and eggshell [21]. The source/type of material used in the production of AC greatly impacts the reactivity of the produced AC and the overall performance of the adsorption process.

Corn cob (CC) is an agro-waste product that is generated in the course of corn processing. In Nigeria, CC is typically considered a useless material because there is no developed use for it. Annually, several million tonnes of corn cobs are disposed of in the environment as waste, posing serious environmental pollution concerns. In 2016/2017, Nigeria produced approximately 10.5 million tonnes of corn [22]. Hence, it is pertinent to develop a research-based utilization channel for this widely available agro-waste product. According to reports, AC produced from CC can effectively be used to remove some wastewater contaminants such as arsenic [23], uranium [24], oil and grease [25], and mercury [26]. The findings of the studies showed that CC meets the criteria of good adsorbent source material, and it is on the heels of this revelation that thermally modified corn cob (TMCC) was considered for the removal of noxious phenol from aqueous solutions in this study.

Until now, the focus of most adsorption studies is on pollutants' removal efficiency, adsorption kinetics, equilibrium isotherms, and thermodynamics. However, the essential parameters necessary for the development and characterization of sorbents and the optimization of the sorption process are the equilibrium isotherms and the isosteric heat of adsorption [27, 28]. While equilibrium adsorption isotherms have been widely studied, studies of the isosteric heats are scarce in the literature. The isosteric heat of adsorption is defined as the heat of adsorption calculated at a fixed amount of the adsorbed compound [28]. It is an essential design parameter in estimating the performance of a sorption process. Information about adsorbent-adsorbate interaction as well as the surface energetic heterogeneity is also obtained from the isosteric heat study [27]. It tells if the adsorption is dominated by a physical process or a chemical process. The complexity of the sorption process taking place at the liquid-solid interfaces necessitates an in-depth study of the isosteric heats.

Other parameters that are important for a comprehensive analysis of an adsorption process and the adsorbent's characteristics whose information is not sufficient in literature for specific adsorption processes like that of phenol uptake onto TMCC are the adsorption mechanism and the point of zero charge of the adsorbent (pH_{pzc}). The study of the adsorption mechanism provides information regarding the sequential steps involved in the removal of pollutants in an adsorption process as well as the rate-determining step. On the other hand, the pH_{pzc} of an adsorbent depicts the pH for which its surface charge is zero [29]. The net surface charge of an adsorbent in wastewater solution can be affected by the existence of H^+ or OH^- in the solution [30]; the analysis of the pH_{pzc} helps us to know how it is affected. It also helps to gain insight on the ionization of functional groups and the way they interact with adsorbate species in solution.

To this end, the focus of this work is to study the IHA, adsorption mechanism, and the pH_{pzc} of TMCC adsorbent for the uptake of phenol from aqueous solutions. To further obtain insight into the adsorption process and intrinsic characteristics connected to the process, the adsorption equilibrium isotherms, thermodynamics, and adsorbent regeneration and reutilization studies were equally carried out. Most of the available reports on the analysis of adsorption equilibrium isotherms focused on the application of the traditional linear transform technique [3]. Due to the reported shortcomings of the linear transform technique [21, 31], the analysis of adsorption equilibrium isotherms was accomplished in this work following the nonlinear regression technique using the solver add-in function available in the Microsoft Excel software.

2. Materials and Methods

2.1. Materials. The CCs (Figure 1) used for the adsorption process were obtained from a neighborhood maize farm in Awka, Nigeria. The chemical reagents (analytical grade) such as phenol, tetraoxophosphoric acid (H_3PO4), and distilled water used were supplied by a Laboratory Chemical dealer at Bridgehead Market, Onitsha, Nigeria.

2.2. Synthesis and Characterization of the Adsorbent. The synthesis and characterization methods of the adsorbent followed a procedure already described in our recent work [2]. Scanning electron microscopy (SEM) and Fourier transform infrared (FTIR) analyses were carried out on the raw and the thermally modified CC samples to gain insight into the samples' surface morphology and functional groups, respectively. The analysis of the physicochemical properties of the produced adsorbent was also performed following the standard methods of the Association of Official Analytical Chemists [32]. The surface area (m^2/g) was determined according to the Brunauer-Emmett-Teller (BET) method as described [2].

2.3. Adsorption Experiments. The efficiency of phenol uptake onto TMCC was carried out using the standard batch adsorption mode. The process parameters were pH (2–10), initial phenol concentration (100–500 mg/l), contact time (3–60 min), TMCC dosage (0.4–2.0 g), and temperature (30–60°C). The contacting of the adsorbate and the adsorbent was realized by agitating the solution from

(a) (b)

Figure 1: Raw corn cob samples: (a) before crushing and grinding and (b) after grinding.

5–60 min at 200 rpm. Phenol removal (in percentage) was calculated using

$$\text{Phenol removal}\,(\%) = \left(\frac{C_0 - C_e}{C_o}\right) \times 100, \quad (1)$$

while the adsorption capacity (q_e) of phenol by TMCC was estimated according to

$$q_e = \frac{(C_0 - C_e)V}{m}, \quad (2)$$

where C_0 and C_e (mg/l) are the initial and equilibrium concentrations of phenol in the liquid phase, respectively. The volume of the phenol solution (l) and the mass of TMCC used (g) are depicted by V and m, respectively, and q_e is the adsorption capacity (mg/g). The equations used for the analyses of the experimental data are summarized in Table 1.

2.4. Determination of the Point of Zero Charge (pH_{pzc}) of the Adsorbent. The pH_{pzc} of TMCC is the pH where its surface potential charge is zero. It was calculated using a method similar to the one described by Harrache et al. [29] and Putra et al. [30]. About 50 ml of NaCl solutions (0.01 M) was put into several Erlenmeyer flasks. The pH of each solution was adjusted with HCl and NaOH to a specified value between 2 and 10. Thereafter, 0.15 g of TMCC was introduced into the flasks. After 24 hours of agitation at room temperature, the final pH of the ensuing solution was determined. The pH_{pzc} is the point at which the curve p H_{final} vs. $pH_{initial}$ crosses the line at $pH_{final} = pH_{initial}$ [30].

3. Results and Discussion

3.1. Characterization of the Adsorbent. Detailed results and interpretation of the physicochemical properties, surface area, and pore size distribution characterization as well as the instrumental analyses (SEM and FTIR) of the TMCC are reported in our recent work [2]. Summarily, the analysis of the physicochemical properties disclosed that TMCC contained fixed carbon (33.47%), moisture content (5.50%), volatile matter (18.01%), bulk density (0.63 g/ml), ash content (5.82%), porosity (0.24), iodine number (888.35 mg/g), and pH (6.30). The thermal modification of the CC provided the AC with enhanced surface area, average pore width, micropore volume, and pore radius of 903.7 m^2/g, 5.55 nm, 0.389 cm^3/g, and 16.20 Å, respectively. SEM images revealed that interspatial pores exist within the matrix of the TMCC, while the result of the FTIR analysis indicated that the key functional groups present in the TMCC were alkyls, alkanes, alkanol, carboxylic acids, esters, ethers, and nitro compounds.

3.2. Effects of Operating Variables on Phenol Adsorption

3.2.1. Effect of Contact Time and Initial Phenol Concentration. The time needed to attain equilibrium is a critical factor in batch adsorption system design. The impact of the contact period on phenol percentage adsorption was investigated at various initial phenol concentrations, as shown in Figure 2(a). The result showed that the adsorption of phenol increased as the contact time increased up to 30 min. After 30 min, increasing the contact time further did not improve phenol adsorption significantly. At the initial stage, the adsorption rate was rapid owing to the adsorption of phenol molecules onto the exterior surface of the adsorbent; thereafter, the molecules entered the interior surface of the adsorbent, a slow process relatively. The initial quicker rates of adsorption can also be attributed to the huge number of adsorption binding sites, and the slower rates at the final moment are due to adsorption site saturation and the realization of equilibrium [45]. Similar results have been reported by Abdelkreem [46] for phenol adsorption using olive mill waste. Generally, an increase in the initial phenol concentration resulted to a decrease in the adsorption efficiency. This is a result of the buildup of phenol molecules on the adsorbent's surface [47].

3.2.2. Effect of Solution pH. One of the most significant variables affecting the output of an adsorption process is the pH of the aqueous solution [45, 48, 49]. The impact of pH level on phenol uptake was investigated at pH levels ranging from 2 to 10, as shown in Figure 2(b). The results show that as the

Table 1: Equations of the isotherm models, mechanism models, thermodynamics, isosteric heat of adsorption, and error functions [33–43].

	Equations	Plot parameters	Equation no.	Source
Equilibrium isotherm models				
Langmuir	$q_e = \frac{q_m K_L C_e}{1 + K_L C_e}$	q_e=adsorption capacity at equilibrium (mg/g) K_L=Langmuir's constant (l/mg) q_m=maximum adsorption capacity (mg/g)	(3)	[33]
	$R_L = \frac{1}{1 + K_L C_o}$	R_L=the separation factor	(4)	
Toth	$q_e = \frac{q_m K_T C_e}{\left[1 + (K_T C_e)^n\right]^{1/n}}$	K_T=Toth's constant (mg/g) n=Toth's isotherm exponent (mg/g)	(5)	[34, 35]
Redlich–Peterson	$q_e = \frac{AC_e}{1 + BC_e^{\beta}}$	A=Redlich–Peterson's constant (l/g) B=constant (l/mg) β=exponent	(6)	[36, 37]
Sips	$q_e = \frac{K_s C_e^{\beta_s}}{1 - a_s C_e^{\beta_s}}$	K_s=Sips' constant (l/g) a_s=monolayer adsorption capacity (mg/g)	(7)	[36]
Adsorption mechanism models				
Intraparticle diffusion	$q_t = K_d t^{1/2} + C$	q_t=adsorption capacity at time, t (mg/g) K_d=intraparticle diffusion constant (mg/g min$^{0.5}$)	(8)	[38]
Boyd	$B_t = -0.4977 - \ln(1 - F)$ $F = 1 - \left(6/\pi^2\right) \exp(-B_t)$; $F = q_t/q_e$	F=fraction of solute adsorbed at any time B_t=Boyd's number (rate parameter)	(10) (11)	[39–41]
Bangham	$\log\left[\log\left(\frac{C_o}{C_o - q_t m}\right)\right] = \log\left(\frac{k_o m}{2.30V}\right) + \alpha \log t$	k_o=Bangham's constant α=Bangham's constant (l^2/g) V=volume of solution (l)	(9)	[39, 41]
Thermodynamics				
Gibbs free energy	$\Delta G^o_{\text{ads}} = -\text{RT}\ln K$	ΔG^o_{ads}=Gibbs free energy (kJ/mol) R=ideal gas constant (R = 8.314 J/mol.K)		
Van't Hoff's equation	$\ln K = \frac{\Delta S^o_{\text{ads}}}{R} - \frac{\Delta H^o_{\text{ads}}}{\text{RT}}$	K=equilibrium constant (l/g) (ΔH^o_{ads})=enthalpy (kJ/mol) (ΔS^o_{ads})=entropy (J/mol.K) T=temperature (K)	(12) (13)	[42] [42]
Isosteric heat of adsorption				
	$d(\text{Ln}C_e) = -\frac{\Delta H_x}{\text{RT}^2} \times dT$ $\text{Ln}C_e = -\frac{\Delta H_x}{\text{RT}} + C$	C_e=equilibrium concentration at constant amount of the adsorbate (mg/l) ΔH_x=isosteric heat of adsorption (kJ/mol)	(14) (15)	[28] [28]
Error functions				
Root-mean-square error (RMSE)	$\sqrt{\frac{1}{N-2}\sum_{i=1}^{N}\left(q_{e,\text{exp}} - q_{e,\text{pred}}\right)^2}$	$q_{e,\text{exp}}$=experimental q_e value $q_{e,\text{pred}}$=model predicted q_e value N=number of observations in the experimental data	(12)	[43]
Chi-squared function (χ^2)	$\sum_{i=1}^{N}\left[\frac{\left(q_{e,\text{exp}} - q_{e,\text{pred}}\right)^2}{q_{e,\text{exp}}}\right]$		(13)	[44]

pH increased from 2 to 6, the adsorption efficiency increased and thereafter decreased. The optimum percentage of phenol removal was achieved at a pH of 6. Some researchers proposed that the pH range of 6 to 8 is optimal for phenol adsorption [47, 50]. At low levels of pH, phenol removal was minimal, because of the existence of hydrogen ions (H +), which are liable for suppressing phenol ionization and, as a result, reducing its sorption on polar solvents [47]. The observed decrease in phenol removal at elevated pH levels (that is at pH levels higher than 6) could be explained by a rise in hydroxide ion (OH-) concentration, which induces a repulse with the negative active sites on the adsorbent, thus lowering phenol uptake [50]. Equally, at high pH, phenolic ions form salts that readily ionize, releasing negative charges on the phenolic group which subsequently inhibit the sorption of phenol ions [47].

3.2.3. Effect of TMCC Dosage. The impact of TMCC dosage on phenol removal efficiency was studied at a dosage range of 0.4 to 2.0 g as shown in Figure 2(c). The efficiency of phenol removal was observed to be directly proportional to TMCC dosage. This is a consequence of the increase in the available active sorption sites as a result of the increased number of sorbents available for the uptake of an equal

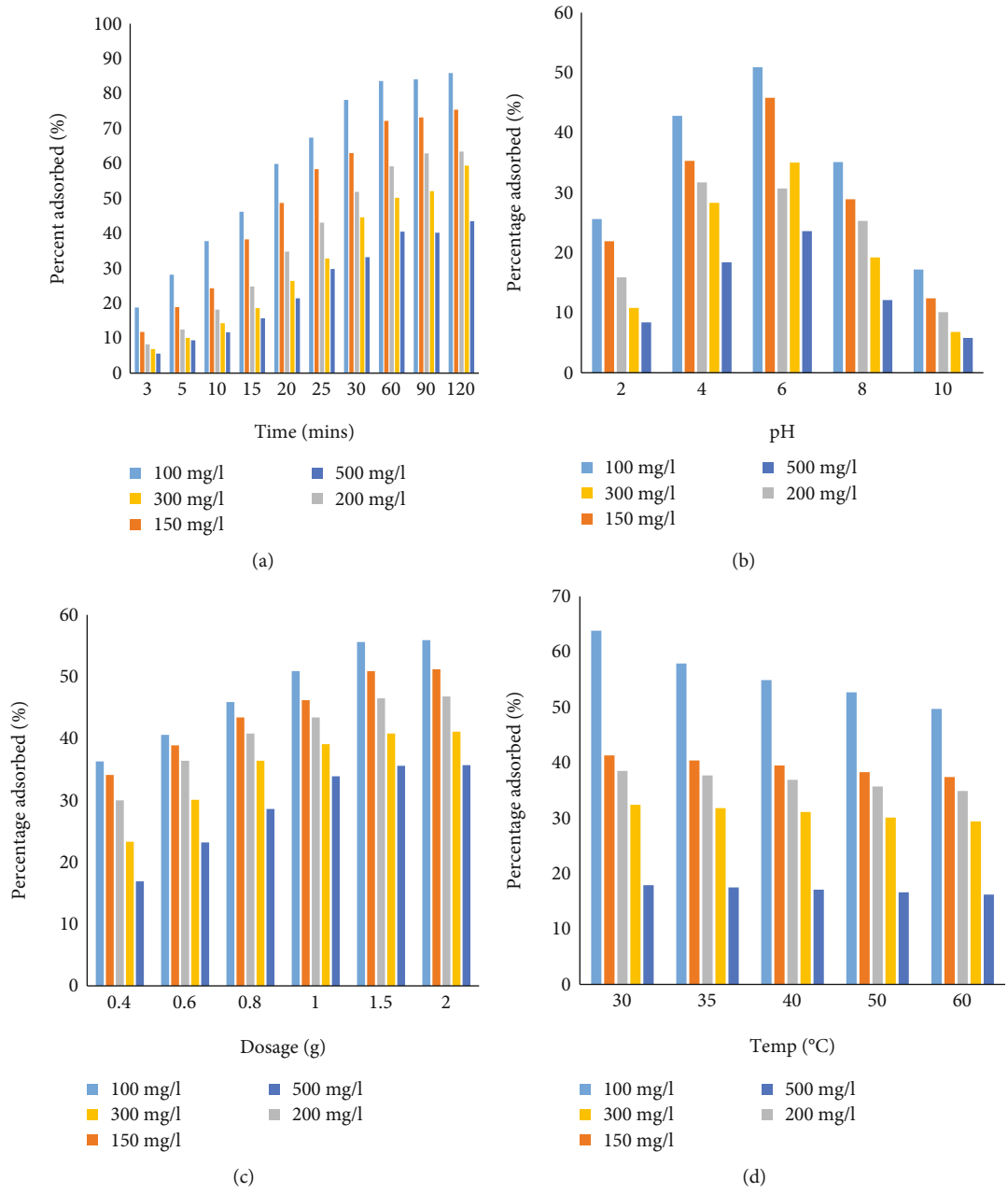

Figure 2: Effects of operating variables on phenol adsorption: (a) effect of contact time and initial phenol concentration, (b) effect of solution pH, (c) effect of adsorbent dosage, and (d) effect of solution temperature.

number of phenolic ions. This result is in concurrence with the works reported by Abdelkreem [46], Uddin et al. [51], and Saravanakumar and Kumar [52] in comparable studies.

3.2.4. Effect of Solution Temperature. Figure 2(d) illustrates the influence of solution temperature on phenol adsorption efficiency. This was studied in a temperature range of 30 to 60°C. From the figure, it can be seen that the efficiency of phenol uptake varies significantly with temperature. The adsorption of phenol increased with a decrease in temperature indicating that a low temperature favors phenol adsorption. This is because as temperature increases, the adsorptive force between the adsorbent's active vacant sites and the adsorbate (phenol ions) is weakened, ultimately leading to a decrease in phenol adsorption efficiency. It has been also suggested that higher temperature enhances the thermal energies of the adsorbate, hence making the attractive force between the phenol species and the adsorbent insufficient to retain the adsorbed molecules at the binding sites [53]. A similar result has been reported by Bazrafshan et al. [54].

3.3. Equilibrium Isotherm Study. The data generated from the experiments were analyzed using the Langmuir, Toth, Sips, and Redlich–Peterson isotherm models. To minimize error distribution, the parameters of the isotherm models were evaluated by the nonlinear regression method using

Table 2: Isotherm parameters for the uptake of phenol onto TMCC.

Isotherm	Parameters	Temperature (°C)				
		30	35	40	50	60
Langmuir	q_m (mg/g)	20.4	20.1	16.6	16.6	12.7
	K_L (l/mg)	0.001	0.001	0.001	0.00093	0.00093
	R^2	0.9986	0.9990	0.9983	0.9991	0.9989
	RMSE	0.01823	0.01773	0.01025	0.01262	0.00767
	χ^2	0.00011	0.00011	0.00004	0.00007	0.00003
Toth	q_m (mg/g)	7.9	7.7	6.6	6.3	4.8
	K_T (mg/g)	0.030	0.030	0.027	0.028	0.034
	n (mg/g)	0.638	0.642	0.645	0.645	0.630
	R^2	0.9969	0.9976	0.9986	0.9989	0.9976
	RMSE	0.01929	0.01943	0.00645	0.00973	0.00799
	χ^2	0.00025	0.00026	0.00003	0.00008	0.00007
Redlich–Peterson	A (l/g)	0.030	0.030	0.025	0.024	0.021
	B (l/mg)	0.23	0.25	0.26	0.26	0.30
	β	0.26	0.25	0.25	0.25	0.27
	R^2	0.9803	0.9989	0.9683	0.9961	0.9751
	RMSE	0.04850	0.01310	0.0311	0.01827	0.02594
	χ^2	1.68798	1.60939	1.55561	0.94391	0.31061
Sips	K_s (l/g)	3.70	3.55	3.10	2.90	2.20
	β_s	0.0098	0.0099	0.0094	0.0091	0.0092
	a_s (mg/g)	0.32	0.34	0.32	0.34	0.35
	R^2	0.9990	0.9957	0.9970	0.9968	0.9993
	RMSE	0.01089	0.02622	0.00960	0.01640	0.00433
	χ^2	0.00008	0.00047	0.00008	0.00023	0.00002

Table 3: Comparison of the regression coefficient (R^2), root-mean-square error (RSME), and Chi-squared test (χ^2) isotherm models.

Regression coefficient/error functions	Isotherm	Temperature (°C)				
		30	35	40	50	60
R^2	Langmuir	0.9986	0.9990	0.9983	0.9991	0.9989
	Toth	0.9969	0.9976	0.9986	0.9989	0.9976
	Redlich–Peterson	0.9803	0.9989	0.9683	0.9961	0.9751
	Sips	0.9990	0.9957	0.9970	0.9968	0.9993
RMSE	Langmuir	0.01823	0.01773	0.01025	0.01262	0.00767
	Toth	0.01929	0.01943	0.00645	0.00973	0.00799
	Redlich–Peterson	0.04850	0.01310	0.0311	0.01827	0.02594
	Sips	0.01089	0.02622	0.00960	0.01640	0.00433
χ^2	Langmuir	0.00011	0.00011	0.00004	0.00007	0.00003
	Toth	0.00025	0.00026	0.00003	0.00008	0.00007
	Redlich–Peterson	1.68798	1.60939	1.55561	0.94391	0.31061
	Sips	0.00008	0.00047	0.00008	0.00023	0.00002

Table 4: Comparison of adsorption capacities of various bioadsorbents for phenol removal from aqueous solutions.

Adsorbent	Adsorption capacity (mg/g)	Reference
TMCC	20.40	Present study
Al-pillared bentonite	1.81	[58]
Thermal bentonite	1.30	[58]
Coal	13.23	[59]
Coke breeze	0.172	[59]
Rice husk	4.508	[59]
Rice husk	0.002	[60]
Rice husk ash	0.886	[60]
Petroleum coke	6.01	[59]
Neutralized red mud	4.127	[61]
Aged-refuse in biofilter	0.597	[62]
Luffa cylindrica	9.25	[63]
Peanut shells	21.00	[64]
Lantana camara (KOH treated)	91.07	[65]

the solver add-in function available in Microsoft Excel software.

The Langmuir model is a simple, semiempirical model that is founded on a kinetic principle. It assumes the following: a homogenous adsorbent surface, adsorbed molecules do not interact, adsorptions follow the same mechanism in all cases, and only a monolayer is formed at the maximum adsorption [33]. The nonlinear representation of the Langmuir model is written as equation (3). The parameters obtained from the nonlinear regression of the Langmuir model are presented in Table 2. As can be seen from the table, both q_m and K_L values increased with a decrease in temperature. The coefficient of determination (R^2) is in the range of 0.9983-0.9991 at different temperature conditions, indicating a good fit. In the validation of the fitness of the Langmuir model in analyzing the adsorption process, the calculated error functions are very low, indicating minimal error distribution. The parameters of the Langmuir model were further expressed with respect to the dimensionless separation factor, R_L represented by equation (4). The value of R_L shows whether the adsorption is favorable ($0 < R_L < 1$), unfavorable ($R_L > 1$), linear ($R_L = 1$), or irreversible ($R_L = 0$). The R_L values obtained at different temperatures and initial concentrations were between 0 and 1, depicting favorable adsorption of phenol onto TMCC. One of the key shortcomings of the Langmuir model is that it does not explain the material's heterogeneity [34].

The Toth isotherm model was established to enhance and remediate the limitations of the Langmuir model [34]. The model provides an adequate description of the heterogeneity of the adsorbent. It is fitting for modeling an assortment of multilayers and heterogeneous adsorption systems [35]. The Toth model is represented by equation (5). The parametric constants evaluated are summarized in Table 2. The R^2 obtained from the model analysis was quite high, varying from 0.9976 to 0.9989, an indication of a good correlation with the adsorption data. The low values of the error parameters affirm that Toth's predicted and actual adsorption capacities were quite comparable. The factor "n" typifies the adsorption system's heterogeneity; if $n = 1$, the model reduces to the Langmuir isotherm; however, if it departs further from unity (1), the system is considered heterogeneous [55]. The "n" values as deduced ranged between 0.630 and 0.645, depicting a heterogeneous surface.

The Redlich–Peterson (R-P) model is an empirical model that incorporates three parameters (A, B, and β). It features elements from both the Freundlich and Langmuir models. The numerator of the model depicts a linear dependence on concentration, while an exponential function at the denominator represents adsorption equilibria over a broad spectrum of concentrations [36, 56, 57]. At high concentration (that is, as the exponent β tends to zero), it tends towards the Freundlich isotherm model, and at low concentration (that is, as the β values are all close to one), it approaches the ideal Langmuir condition [37]. The Redlich–Peterson model is represented by equation (6). The derived parameters of the Redlich-Peterson isotherm are presented in Table 2. The R-P isotherm constant A was observed to decrease as the temperature increased. The coefficient of determination is in the range of 0.9683 to 0.9989, indicating a good fit.

The Sips model is a hybrid of the Langmuir and Freundlich models devised for estimating heterogeneous adsorption systems and surmounting the Freundlich model's limitation associated with rising adsorbate concentration [36]. When adsorbate concentrations are low, it tends towards the Freundlich isotherm; and when the concentrations are high, a monolayer adsorption capacity typical of the Langmuir isotherm is predicted [36, 56, 57]. The Sips model is described by equation (7). Table 2 displays the values of various parameters of the Sips isotherm estimated at different temperature values. The $K_s$values decreased as temperature increased, in the range of 2.2 to 3.7 l/g. The isotherm exponent, β_s, and the monolayer adsorption capacity, a_s, showed no linear relationship with temperature. High R^2 values (ranging from 0.9957 to 0.9993) and low error parameter values indicate a good correlation between the actual and Sips model data. A direct comparison of the suitability of the models in the analysis of the adsorption data has been provided in terms of the regression coefficient (R^2), root-mean-square error (RSME), and Chi-squared test (χ^2) (see Table 3). The decreasing order of the fitness of the models is the Sips, Langmuir, Toth, and Redlich–Peterson models. Furthermore, comparison of this work's maximum adsorption capacity and those reported for other bioadsorbents is presented in Table 4.

3.4. Point of Zero Charge (pH_{pzc}). The pH_{pzc} of an adsorbent is the pH at the point where its surface charge is zero [29]. The existence of H^+ or OH^- in wastewater solutions may change the net surface charge of adsorbents [30]. The

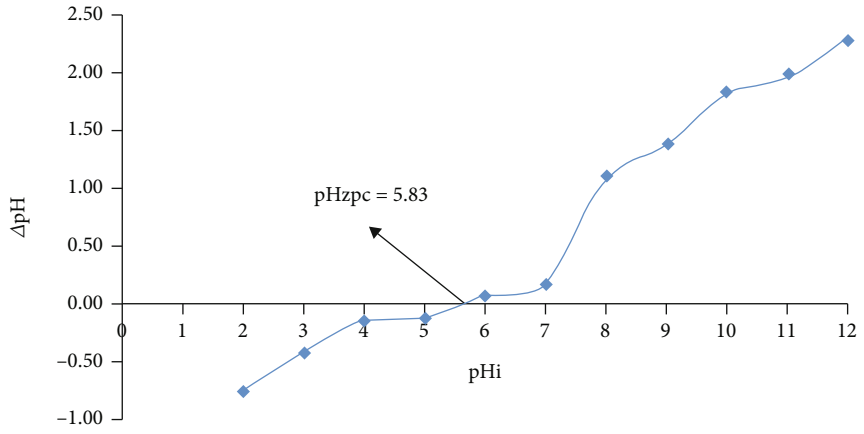

Figure 3: Point of zero charge for phenol adsorption onto TMCC.

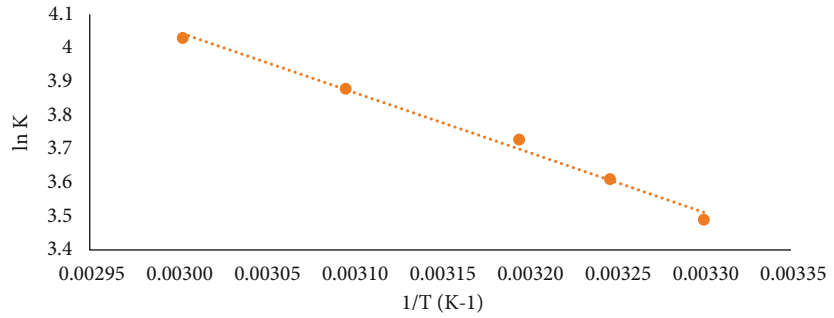

Figure 4: Van't Hoff's plot for thermodynamic analysis.

Table 5: Adsorption thermodynamic parameters.

T (°C)	T (K)	ΔG^o_{ads} (kJ/mol)	ΔH^o_{ads} (kJ/mol)	ΔS^o_{ads} (J/mol.K)
30	303	-8.792	14.834	78.154
35	308	-9.246		
40	313	-9.702		
50	323	-10.417		
60	333	-11.157		

analysis of the pH_{pzc} helps to gain information on the ionization of functional groups and the way they interact with adsorbate species in solution. If a solution's pH is higher than its pH_{pzc}, the surface functional groups on adsorbents will be protonated by the excess H^+ ions; if it is lower than its pH_{pzc}, the surface functional groups will be deprotonated by the OH^- ions present in the solution [30]. In other words, if the solution pH is above the pH_{pzc}, the sorbent surface interacts with the positive species since this indicates that its surface charge at that condition is negative, whereas at pH lower than pH_{pzc}, the interaction will be with the negative species because it is possessing a positive charge. The point of zero charge of phenol uptake onto TMCC is 5.83, and the plot is illustrated in Figure 3. In this study, optimum phenol uptake onto TMCC was obtained at a pH of 6 which is slightly higher than the pH_{pzc}. This is an indication that the TMCC surface is not negatively charged at this pH.

3.5. Adsorption Thermodynamics. For an enhanced understanding of the adsorption process and the influence of temperature on it, the following thermodynamic properties, such as changes in standard Gibbs free energy (ΔG^o_{ads}), enthalpy (ΔH^o_{ads}), and entropy (ΔS^o_{ads}), were estimated using equations (12) and (13). The values of ΔH^o_{ads} and ΔS^o_{ads} were deduced from the plots of ln K versus $1/T$ (Figure 4) and presented in Table 5. The ΔG^o_{ads} values ranged from -8.792 to -11.157 kJ/mol at 303 to 333 K. The ΔH^o_{ads} and ΔS^o_{ads} values are 14.834 kJ/mol and 78.154 J/mol.K, respectively. The negative values of ΔG^o_{ads} at varying temperatures depict a spontaneous adsorption process. The adsorption process with ΔG^o_{ads} in the range of -80 to -400 kJ/mol depicts a chemisorption process [42], but, since the ΔG^o_{ads} obtained in this work is in the range of -8.792 to -11.157 kJ/mol, it indicates a physisorption-dominated mechanism, in agreement with the experimental result which suggested that adsorption is rapid and is inversely proportional with temperature. The positive value of ΔH^o_{ads} indicates the endothermic nature of the adsorption process. Also, since ΔH^o_{ads} is <40 kJ/mol, a physical adsorption process is further suggested [42]. The

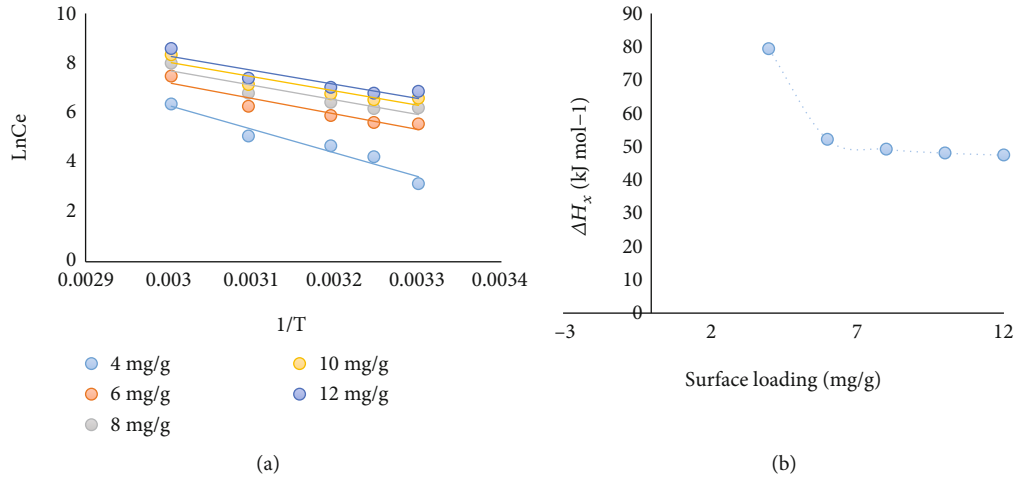

Figure 5: (a) Plots of LnC_e against 1/T for the determination of ΔH_x. (b) Plot of ΔH_x against surface loading.

Table 6: Isosteric heat of adsorption parameters.

q_e (mg/g)	ΔH_x (kJ/Mol)	R^2
4	79.38	0.9408
6	52.14	0.8938
8	49.20	0.8654
10	48.05	0.8526
12	47.43	0.8453

positive value of $\Delta S^o_{\mathrm{ads}}$ reflects the favorable affinity phenol has for TMCC and the increasing degree of randomness at the solid-solution interface during the adsorption of phenol ions onto TMCC adsorbent.

3.6. Isosteric Heat of Adsorption. The isosteric heat of adsorption (ΔH_x, kJ/mol) is the heat of adsorption deduced at a fixed amount of the adsorbed compound [28, 66]. Information about isosteric heat of adsorption is critical for the adsorption plant and process design. The isosteric heats at fixed surface coverage ($q_e = 4, 6, 8, 10, 12$ mg/g) were estimated using the Clausius–Clapeyron equation, equation (14), expanded as equation (15). The equilibrium concentration (C_e) values at a constant amount of phenol adsorbed were deduced from the isotherm data at varying temperatures. The ΔH_x values were calculated from the slope of the linear plot of LnC_e against $1/T$ (Figure 5(a)). Table 6 presents the linear regression coefficients and the ΔH_x values as calculated. The ΔH_x value should be less than 80 kJ/mol for physical adsorption and between 80 and 400 kJ/mol for chemical adsorption [28, 66]. The ΔH_x values obtained in this study are between 47.43 and 79.38 kJ/mol signifying that phenol adsorption onto TMCC is dominated by a physical process, validating the thermodynamic results.

Figure 5(b) illustrates how ΔH_x varies with q_e (surface loading). It can be deduced from the figure that ΔH_x decreased as the q_e values increased, indicating that TMCC is associated with energetically heterogeneous surfaces [27, 28]. The nature of the variation of ΔH_x with q_e can be credited to adsorbate-adsorbent interaction proceeded by adsorbate-adsorbate interaction [28, 45]. At low values of surface loading, adsorbent-adsorbate interaction dominates resulting in high ΔH_x, and as the surface loading increases, adsorbate-adsorbate interaction dominates [27].

3.7. Mechanism Studies. The mechanism of adsorption is generally considered to follow three steps, one or any combination of which can be the rate-controlling mechanism [67, 68]: (i) film diffusion, (ii) pore diffusion (i.e., external mass transfer), and (iii) intraparticle transport diffusion. The adsorption mechanism of phenol uptake onto TMCC was studied via the application of the intraparticle diffusion, Bangham, and Boyd models.

The intraparticle diffusion plot is one of the prominent techniques for assessing the mechanism involved in an adsorption process. It expresses the relationship between the adsorption capacity (q_t) and time $t^{1/2}$ as depicted by equation (8) [38]. The model parameters are depicted in Table 7. The high R^2 values indicated the presence of intraparticle diffusion in the adsorption process. As depicted by the regression coefficients, the plot points were not entirely linear over the whole operational time interval, indicating that the adsorption was influenced by more than one process. Also, if the intraparticle diffusion were the sole rate-controlling step, the plot would pass through the origin [67]; however, because the plot failed to transit through the origin (as depicted by the C values in Table 7), intraparticle diffusion, while implicated in the adsorption process, does not constitute the rate-controlling step. The C values represent the thickness of the boundary layer; a bigger intercept represents a greater involvement of surface adsorption in the rate-controlling step [69].

Another important model that helps to gain a better understanding of the adsorption mechanism is Boyd's model. Boyd's film-diffusion model was initially suggested for intraparticle diffusion in a spherical particle [40]. Equations (10) and (11) are used for the analysis of Boyd's model [39–41]. The plot of the calculated rate parameter B_t versus

Table 7: Adsorption mechanism model parameters for phenol uptake onto TMCC.

Mechanism model	Concentration (mg/l)				
	100	150	200	300	500
Intraparticle diffusion					
K_d (mg/g min$^{-0.5}$)	0.803	1.033	1.173	1.518	1.092
C (intercept)	0.375	0.483	0.482	0.529	1.092
R^2	0.9755	0.9754	0.9591	0.9483	0.9742
Boyd					
Intercept	-1.1666	-1.0527	-0.9793	-1.0094	-0.7714
R^2	0.8147	0.8879	0.9410	0.9130	0.9566
Bangham					
k_o	118.79	117.99	117.42	117.19	116.04
α (l^2/g)	0.0177	0.0165	0.0147	0.0131	0.0142
R^2	0.7192	0.7776	0.8391	0.8465	0.9018

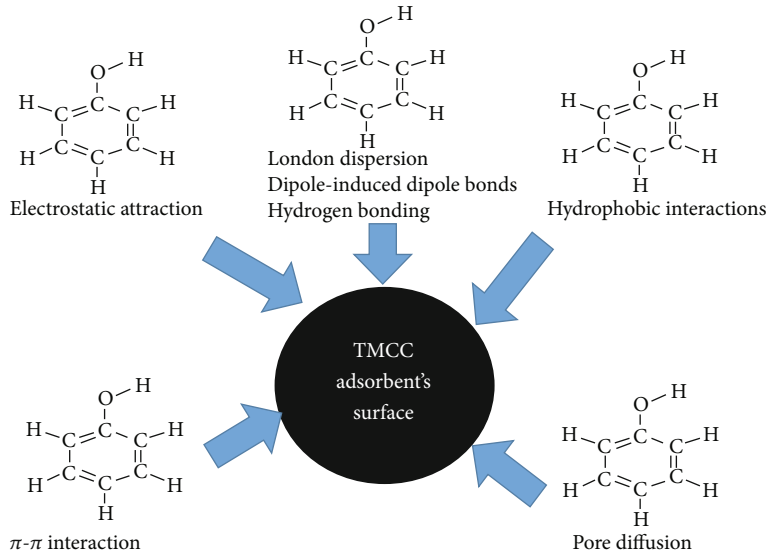

Figure 6: Summary of the adsorption mechanism of phenol onto TMCC at optimum pH.

time t depicts Boyd's model. The plots were observed to be linear with a high coefficient of determination ($R^2 > 0.90$ in most cases) indicating the participation of film diffusion in the mechanism [39, 70]. The fact that the plot did not pass through the origin (as illustrated by the intercept values in Table 7) indicates the involvement of a second mass transfer mechanism (external mass transfer) [40]. Similar outcomes have been reported by Martins et al. [70] and Üner et al. [39] in similar studies.

According to Bangham's model, the diffusion of phenol molecules into the pore spaces of the adsorbent makes a significant contribution to the rate-controlling step [39, 71]. It is described by equation (36) [39, 41]. The plot of log [log ($C_o/C_o - q_t m$)] against time t gave a straight line with R^2 in the range of 0.7192 and 0.9018 as shown in Table 7. This indicates the occurrence of pore diffusion and affirmed the presumption of Bangham's model.

Further, as indicated by the thermodynamics analysis, physisorption as well as the van der Waal and electrostatic interactions are also involved in the phenol uptake. Phenol has a pKa of 9.89 [72], and below this pH, it is protonated to its cationic form. An important mechanism of adsorption is the electrostatic attraction between phenol and the adsorbent's negatively charged surface (observed from the pH_{ZPC} study). Weak hydrogen bonding and pore diffusion also play a role in phenol adsorption (to a lesser extent). Hydrogen bonding allows water molecules to be adsorbed on the surface oxygen groups. Because the adsorbate's alkyl hydrogens can interact with the molecules on the adsorbent's functional groups such as oxygen, hydrogen bonding is established (corroborated by the FTIR). Hydrogen bonds are a sort of dipole-dipole moment and a weak partial intermolecular link [73]. The FTIR study verified functional groups such as C-O, C=O, and -OH. Phenol is a benzene-like polycyclic

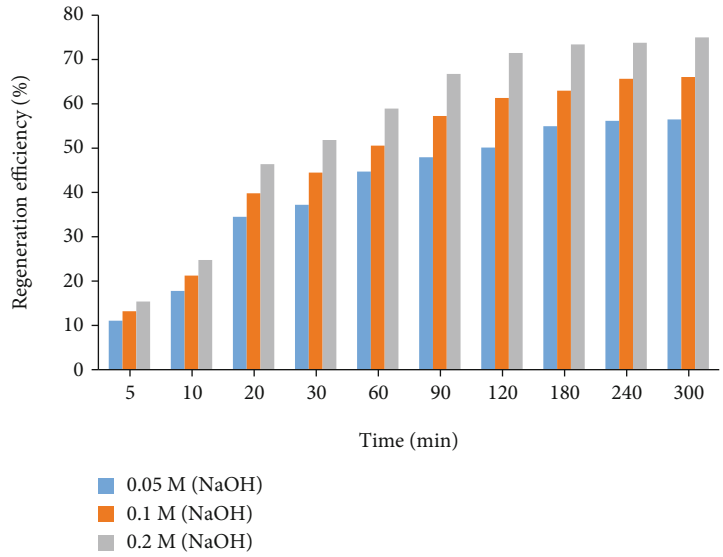

Figure 7: Reuse of regenerated adsorbent using different concentrations of NaOH.

aromatic molecule. The benzene rings cause a donor-acceptor connection and the phenol to stack onto the adsorbent [74]. That is, the carbon surface's electron acceptors and basic sites serve as donors [72]. As a result, the π-π electron-donor interaction is a contributing factor. The hydrophobic interactions are thought to contribute to phenol adsorption, which is another rationale for the higher adsorption of substituted phenols [75]. Conclusively, electrostatic attraction, hydrophobic interactions, π-π electron-donor interaction, hydrogen bonding, the van der Waal interactions (may be London dispersion and dipole-induced dipole bonds), and pore diffusion played quite a significant part in the phenol adsorption process as illustrated in Figure 6.

3.8. Adsorbent Regeneration and Reutilization Studies. Adsorbent regeneration tests were carried out to assess the potentiality of reusing the adsorbent for other adsorption activities and also to render the process more economically attractive. The used adsorbents were treated with sodium hydroxide (NaOH) solution. This was accomplished using the batch method of operations employing varying concentrations of sodium hydroxide (NaOH) solution. Sodium hydroxide was selected because it has been reported as the most effective desorbing/regenerating agent [76–78]. The results depicted in Figure 7 indicate that after approximately 300 minutes, the adsorption efficiency for spent TMCC was 56.48%, 66.05%, and 74.99% using 0.05 M, 0.1 M, and 0.2 M NaOH solutions, respectively. The adsorption performance was found to be relatively within these ranges for about three cycles of regeneration before declining significantly to the point where it was no longer economically feasible. This shows that TMCC adsorbent could be retrieved and reused in the aqueous phenol adsorption.

4. Conclusion

The current study demonstrates that CC, which is typically discarded as waste products, can be effectually used as raw material in the production of adsorbents for the uptake of phenol from aqueous solutions. The nonlinear regression technique was used to evaluate the equilibrium isotherms. The fitness of the isotherm models to the experimental data was in this decreasing order—Sips', Langmuir's, Toth's, and Redlich–Peterson's models. The uptake of phenol onto TMCC is favorably influenced by a decrease in initial phenol concentration and temperature and an increase in TMCC dosage and contact time. Phenol removal increased with pH from 2 to 6 and decreased thereafter. The negative values of $\Delta G^{o}_{\text{ads}}$ at varying temperatures depict a spontaneous adsorption process. The isosteric heats of adsorption were estimated using the Clausius–Clapeyron equation, and it confirmed that the adsorption process is a physical process dominated by the van der Waals interactions. The values of the isosteres decreased with an increase in surface coverage, signifying a heterogeneous surface. The transport mechanisms depicted in the process were intraparticle, film, and pore diffusion mechanisms. Furthermore, the electrostatic attraction, π-π electron-donor interaction, and hydrogen bonding were also involved in the phenol adsorption. The point of zero charge of TMCC was 5.83, slightly lower than the optimum pH of the adsorption process. These results provided detailed information regarding the equilibrium characteristics, adsorption mechanism, energy and surface interactions, and the point of zero charge of TMCC for the uptake of phenol.

Data Availability

No data were used to support this study. All data generated or analyzed during this study are included in this article.

Conflicts of Interest

There are no conflicts of interest to declare.

Authors' Contributions

All authors contributed to the study's conception and design. Material preparation, data collection, and analysis were performed by Ositadinma Chamberlain Iheanacho, Joseph Tagbo Nwabanne, and Chijioke Elijah Onu. The first draft of the manuscript was written by Christopher Chiedozie Obi. Manuscript review and editing were carried out by Chinenye Adaobi Igwegbe and Irvan Dahlan. All authors read and approved the final manuscript.

Acknowledgments

The authors thankfully acknowledge the Department of Chemical Engineering, Nnamdi Azikiwe University, Awka, Nigeria, for making available their laboratory facilities for the experiments.

References

[1] J. T. Nwabanne, O. C. Iheanacho, C. C. Obi, and C. E. Onu, "Linear and nonlinear kinetics analysis and adsorption characteristics of packed bed column for phenol removal using rice husk-activated carbon," *Applied Water Science*, vol. 12, no. 5, 2022.

[2] O. C. Iheanacho, J. T. Nwabanne, C. C. Obi, and C. E. Onu, "Packed bed column adsorption of phenol onto corn cob activated carbon: linear and nonlinear kinetics modeling," *South African Journal of Chemical Engineering*, vol. 36, pp. 80–93, 2021.

[3] R. R. Karri, J. N. Sahu, and N. S. Jayakumar, "Optimal isotherm parameters for phenol adsorption from aqueous solutions onto coconut shell based activated carbon: error analysis of linear and non-linear methods," *Journal of the Taiwan Institute of Chemical Engineers*, vol. 80, pp. 472–487, 2017.

[4] S. G. Thakurta, M. Aakula, J. Chakrabarty, and S. Dutta, "Bioremediation of phenol from synthetic and real wastewater using Leptolyngbya sp.: a comparison and assessment of lipid production," *3 Biotech*, vol. 8, no. 4, pp. 1–10, 2018.

[5] L. G. C. Villegas, N. Mashhadi, M. Chen, D. Mukherjee, K. E. Taylor, and N. Biswas, "A short review of techniques for phenol removal from wastewater," *Current Pollution Reports*, vol. 2, no. 3, pp. 157–167, 2016.

[6] M. Ghaljahi, S. Rahdar, S. Z. Almasi, S. Ahmadi, and C. A. Igwegbe, "Survey dataset on the externalizing self-esteem and gender effects on self- esteem subscales of students in Zabol University of Medical Sciences, Iran," *Data in Brief*, vol. 21, pp. 407–413, 2018.

[7] K. Saini, B. Biswas, A. Kumar, A. Sahoo, J. Kumar, and T. Bhaskar, "Screening of sugarcane bagasse-derived biochar for phenol adsorption: optimization study using response surface methodology," *International journal of Environmental Science and Technology*, vol. 19, no. 9, pp. 8797–8810, 2022.

[8] Y. Han, N. Wang, X. Guo, T. Jiao, and H. Ding, "Influence of ultrasound on the adsorption of single-walled carbon nanotubes to phenol: a study by molecular dynamics simulation and experiment," *Chemical Engineering Journal*, vol. 427, article 131819, 2022.

[9] D. Feng, D. Guo, Y. Zhang et al., "Functionalized construction of biochar with hierarchical pore structures and surface O-/N-containing groups for phenol adsorption," *Chemical Engineering Journal*, vol. 410, article 127707, 2021.

[10] Y. Dehmani, H. Lgaz, A. A. Alrashdi, T. Lamhasni, S. Abouarnadasse, and I.-M. Chung, "Phenol adsorption mechanism on the zinc oxide surface: experimental, cluster DFT calculations, and molecular dynamics simulations," *Journal of Molecular Liquids*, vol. 324, article 114993, 2021.

[11] J. Zhang, L. Qin, Y. Yang, and X. Liu, "Porous carbon nanospheres aerogel based molecularly imprinted polymer for efficient phenol adsorption and removal from wastewater," *Separation and Purification Technology*, vol. 274, article 119029, 2021.

[12] C. A. Igwegbe, A. E. Al-Rawajfeh, H. I. Al-Itawi et al., "Utilization of calcined gypsum in water and wastewater treatment: removal of phenol," *Journal of Ecological Engineering*, vol. 20, no. 7, pp. 1–10, 2019.

[13] M. Bhowmik, A. Debnath, and B. Saha, "Scale-up design and treatment cost analysis for abatement of hexavalent chromium and metanil yellow dye from aqueous solution using mixed phase CaFe2O4 and ZrO2 nanocomposite," *International Journal of Environmental Research*, vol. 16, no. 5, 2022.

[14] B. Saha, A. Debnath, and B. Saha, "Fabrication of PANI@Fe–Mn–Zr hybrid material and assessments in sono-assisted adsorption of methyl red dye: Uptake performance and response surface optimization," *Journal of the Indian Chemical Society*, vol. 99, no. 9, article 100635, 2022.

[15] P. Das and A. Debnath, "Fabrication of MgFe2O4/polyaniline nanocomposite for amputation of methyl red dye from water: isotherm modeling, kinetic and cost analysis," *Journal of Dispersion Science and Technology*, pp. 1–12, 2022.

[16] C. E. Onu, J. T. Nwabanne, P. E. Ohale, and C. O. Asadu, "Comparative analysis of RSM, ANN and ANFIS and the mechanistic modeling in eriochrome black-T dye adsorption using modified clay," *South African Journal of Chemical Engineering*, vol. 36, pp. 24–42, 2021.

[17] M. O. Aremu, A. O. Arinkoola, I. A. Olowonyo, and K. K. Salam, "Improved phenol sequestration from aqueous solution using silver nanoparticle modified palm kernel shell activated carbon," *Heliyon*, vol. 6, no. 7, article e04492, 2020.

[18] D. M. Naguib and N. M. Badawy, "Phenol removal from wastewater using waste products," *Journal of Environmental Chemical Engineering*, vol. 8, no. 1, article 103592, 2020.

[19] V. Srihari and A. Das, "The kinetic and thermodynamic studies of phenol-sorption onto three agro-based carbons," *Desalination*, vol. 225, no. 1-3, pp. 220–234, 2008.

[20] M. Achak, A. Hafidi, L. Mandi, and N. Ouazzani, "Removal of phenolic compounds from olive mill wastewater by adsorption onto wheat bran," *Desalination and Water Treatment*, vol. 52, no. 13-15, pp. 2875–2885, 2014.

[21] L. Giraldo and J. C. Moreno-Piraján, "Study of adsorption of phenol on activated carbons obtained from eggshells," *Journal of Analytical and Applied Pyrolysis*, vol. 106, pp. 41–47, 2014.

[22] A. Girei, N. Saingbe, S. Ohen, and K. Umar, "Economics of small-scale maize production in Toto local government area, Nasarawa state, Nigeria," *Agrosearch*, vol. 18, no. 1, pp. 90–104, 2018.

[23] M. B. Shakoor, N. K. Niazi, I. Bibi et al., "Exploring the arsenic removal potential of various biosorbents from water," *Environment International*, vol. 123, pp. 567–579, 2019.

[24] M. A. Mahmoud, "Kinetics studies of uranium sorption by powdered corn cob in batch and fixed bed system," *Journal of Advanced Research*, vol. 7, no. 1, pp. 79–87, 2016.

[25] J. O. Ighalo, C. A. Igwegbe, C. O. Aniagor, and S. N. Oba, "A review of methods for the removal of penicillins from water," *Journal of Water Process Engineering*, vol. 39, article 101886, 2021.

[26] X.-L. Duan, C.-G. Yuan, T.-T. Jing, and X.-D. Yuan, "Removal of elemental mercury using large surface area micro-porous corn cob activated carbon by zinc chloride activation," *Fuel*, vol. 239, pp. 830–840, 2019.

[27] V. C. Srivastava, I. D. Mall, and I. M. Mishra, "Adsorption thermodynamics and isosteric heat of adsorption of toxic metal ions onto bagasse fly ash (BFA) and rice husk ash (RHA)," *Chemical Engineering Journal*, vol. 132, no. 1-3, pp. 267–278, 2007.

[28] M. Elmiz, K. Essifi, D. Berraaouan, S. Salhi, and A. Tahani, "Adsorption thermodynamics and isosteric heat of adsorption of thymol onto sodic, pillared and organic bentonite," *Mediterranean Journal of Chemistry*, vol. 8, no. 6, pp. 494–504, 2019.

[29] Z. Harrache, M. Abbas, T. Aksil, and M. Trari, "Thermodynamic and kinetics studies on adsorption of indigo carmine from aqueous solution by activated carbon," *Microchemical Journal*, vol. 144, pp. 180–189, 2019.

[30] E. K. Putra, R. Pranowo, J. Sunarso, N. Indraswati, and S. Ismadji, "Performance of activated carbon and bentonite for adsorption of amoxicillin from wastewater: mechanisms, isotherms and kinetics," *Water Research*, vol. 43, no. 9, pp. 2419–2430, 2009.

[31] H. T. Hamad, "Removal of phenol and inorganic metals from wastewater using activated ceramic," *Journal of King Saud University - Engineering Sciences*, vol. 33, no. 4, pp. 221–226, 2021.

[32] W. Horwitz and G. Latimer, *Official Methods of Analysis of AOAC 18*, AOAC International, Gaithersburg, Md, 2005.

[33] V. Njoku, E. Oguzie, C. Obi, O. Bello, and A. Ayuk, "Adsorption of copper (II) and lead (II) from aqueous solutions onto a Nigerian natural clay," *Australian Journal of Basic and Applied Sciences*, vol. 5, no. 5, pp. 346–353, 2011.

[34] J. Abdulsalam, J. Mulopo, S. O. Bada, and B. Oboirien, "Equilibria and Isosteric Heat of Adsorption of Methane on Activated Carbons Derived from South African Coal Discards," *ACS Omega*, vol. 5, no. 50, pp. 32530–32539, 2020.

[35] T. Benzaoui, A. Selatnia, and D. Djabali, "Adsorption of copper (II) ions from aqueous solution using bottom ash of expired drugs incineration," *Adsorption Science & Technology*, vol. 36, no. 1-2, pp. 114–129, 2018.

[36] K. Y. Foo and B. H. Hameed, "Insights into the modeling of adsorption isotherm systems," *Chemical Engineering Journal*, vol. 156, no. 1, pp. 2–10, 2010.

[37] L. Jossens, J. Prausnitz, W. Fritz, E. Schlünder, and A. Myers, "Thermodynamics of multi-solute adsorption from dilute aqueous solutions," *Chemical Engineering Science*, vol. 33, no. 8, pp. 1097–1106, 1978.

[38] A. Okewale, K. Babayemi, and A. Olalekan, "Adsorption isotherms and kinetics models of starchy adsorbents on uptake of water from ethanol–water systems," *International Journal of Applied Science and Technology*, vol. 3, no. 1, pp. 35–42, 2013.

[39] O. Üner, Ü. Geçgel, and Y. Bayrak, "Adsorption of methylene blue by an efficient activated carbon prepared from Citrullus lanatus rind: kinetic, isotherm, thermodynamic, and mechanism analysis," *Water, Air, & Soil Pollution*, vol. 227, no. 7, 2016.

[40] I. Tsibranska and E. Hristova, "Comparison of different kinetic models for adsorption of heavy metals onto activated carbon from apricot stones," *Bulgarian Chemical Communications*, vol. 43, no. 3, pp. 370–377, 2011.

[41] A. O. Dada, F. A. Adekola, and E. O. Odebunmi, "Kinetics, mechanism, isotherm and thermodynamic studies of liquid phase adsorption of Pb2+ onto wood activated carbon supported zerovalent iron (WAC-ZVI) nanocomposite," *Cogent Chemistry*, vol. 3, no. 1, article 1351653, 2017.

[42] N. N. Nassar, "Kinetics, mechanistic, equilibrium, and thermodynamic studies on the adsorption of acid red dye from wastewater by γ-Fe2O3nanoadsorbents," *Separation Science and Technology*, vol. 45, no. 8, pp. 1092–1103, 2010.

[43] M. R. Samarghandi, M. Hadi, S. Moayedi, and F. Barjasteh Askari, "Two-parameter isotherms of methyl orange sorption by pinecone derived activated carbon," *Iranian Journal of Environmental Health Science & Engineering*, vol. 6, no. 4, pp. 285–294, 2009.

[44] M. Hossain, H. Ngo, and W. Guo, "Introductory of Microsoft Excel SOLVER Function-Spreadsheet Method for Isotherm and Kinetics Modelling of Metals Biosorption in Water and Wastewater," *Journal of Water Sustainability*, vol. 4, pp. 223–237, 2013.

[45] S. Chowdhury, R. Mishra, P. Saha, and P. Kushwaha, "Adsorption thermodynamics, kinetics and isosteric heat of adsorption of malachite green onto chemically modified rice husk," *Desalination*, vol. 265, no. 1-3, pp. 159–168, 2011.

[46] M. Abdelkreem, "Adsorption of phenol from industrial wastewater using olive mill waste," *APCBEE Procedia*, vol. 5, pp. 349–357, 2013.

[47] I. H. Dakhil, "Removal of phenol from industrial wastewater using sawdust," *International Journal of Engineering Science*, vol. 3, no. 1, pp. 25–31, 2013.

[48] G. Crini, H. N. Peindy, F. Gimbert, and C. Robert, "Removal of C.I. basic green 4 (malachite green) from aqueous solutions by adsorption using cyclodextrin-based adsorbent: kinetic and equilibrium studies," *Separation and Purification Technology*, vol. 53, no. 1, pp. 97–110, 2007.

[49] P. Djomgoue, M. Siewe, E. Djoufac, P. Kenfack, and D. Njopwouo, "Surface modification of Cameroonian magnetite rich clay with Eriochrome black T. application for adsorption of nickel in aqueous solution," *Applied Surface Science*, vol. 258, no. 19, pp. 7470–7479, 2012.

[50] M. Akl, M. B. Dawy, and A. A. Serage, "Efficient removal of phenol from water samples using sugarcane bagasse based activated carbon," *Journal of Analytical & Bioanalytical Techniques*, vol. 5, no. 2, pp. 1–12, 2014.

[51] M. Uddin, M. Islam, and M. Abedin, "Adsorption of phenol from aqueous solution by water hyacinth ash," *ARPN Journal of engineering and applied sciences*, vol. 2, no. 2, pp. 11–17, 2007.

[52] K. Saravanakumar and A. Kumar, "Removal of phenol from aqueous solution by adsorption using zeolite," *African Journal of Agricultural Research*, vol. 8, no. 23, pp. 2965–2969, 2013.

[53] D. Jadhav and A. Vanjara, "Removal of Phenol from Wastewater Using Sawdust, Polymerized Sawdust and Sawdust Carbon," *Indian Journal of Chemical Technology*, vol. 11, pp. 35–41, 2004.

[54] E. Bazrafshan, P. Amirian, A. H. Mahvi, and A. Ansari-Moghaddam, "Application of adsorption process for phenolic compounds removal from aqueous environments: a systematic

review," *Global NEST Journal*, vol. 18, no. 1, pp. 146–163, 2016.

[55] T. J. Behbahani and Z. J. Behbahani, "A new study on asphaltene adsorption in porous media," *Petroleum and Coal*, vol. 56, no. 5, pp. 459–466, 2014.

[56] H. Masoumi, A. Ghaemi, and H. Ghanadzadeh Gilani, "Exploiting the performance of hyper-cross-linked polystyrene for removal of multi-component heavy metal ions from wastewaters," *Journal of Environmental Chemical Engineering*, vol. 9, no. 4, article 105724, 2021.

[57] M. Hadi, G. McKay, M. R. Samarghandi, A. Maleki, and M. Solaimany Aminabad, "Prediction of optimum adsorption isotherm: comparison of chi-square and log-likelihood statistics," *Desalination and Water Treatment*, vol. 49, no. 1-3, pp. 81–94, 2012.

[58] S. Al-Asheh, F. Banat, and L. Abu-Aitah, "Adsorption of phenol using different types of activated bentonites," *Separation and Purification Technology*, vol. 33, no. 1, pp. 1–10, 2003.

[59] M. Ahmaruzzaman and D. Sharma, "Adsorption of phenols from wastewater," *Journal of Colloid and Interface Science*, vol. 287, no. 1, pp. 14–24, 2005.

[60] A. Mahvi, A. Maleki, and A. Eslami, "Potential of Rice Husk and Rice Husk Ash for Phenol Removal in Aqueous Systems," vol. 1, no. 4, pp. 321–326, 2004.

[61] A. Tor, Y. Cengeloglu, M. E. Aydin, and M. Ersoz, "Removal of phenol from aqueous phase by using neutralized red mud," *Journal of Colloid and Interface Science*, vol. 300, no. 2, pp. 498–503, 2006.

[62] C. Xiaoli and Z. Youcai, "Adsorption of phenolic compound by aged-refuse," *Journal of Hazardous Materials*, vol. 137, no. 1, pp. 410–417, 2006.

[63] O. Abdelwahab and N. Amin, "Adsorption of phenol from aqueous solutions by *Luffa cylindrica* fibers: kinetics, isotherm and thermodynamic studies," *The Egyptian Journal of Aquatic Research*, vol. 39, no. 4, pp. 215–223, 2013.

[64] B. M. Villar da Gama, G. E. do Nascimento, D. C. S. Sales, J. M. Rodríguez-Díaz, C. M. B. de Menezes Barbosa, and M. M. M. B. Duarte, "Mono and binary component adsorption of phenol and cadmium using adsorbent derived from peanut shells," *Journal of Cleaner Production*, vol. 201, pp. 219–228, 2018.

[65] C. Girish and V. Ramachandra Murty, "Adsorption of phenol from aqueous solution using *Lantana camara*, forest waste: kinetics, isotherm, and thermodynamic studies," *International scholarly research notices*, vol. 2014, Article ID 201626, 16 pages, 2014.

[66] P. Saha and S. Chowdhury, "Insight into adsorption thermodynamics," *Thermodynamics*, vol. 16, pp. 349–364, 2011.

[67] W. H. Cheung, Y. S. Szeto, and G. McKay, "Intraparticle diffusion processes during acid dye adsorption onto chitosan," *Bioresource Technology*, vol. 98, no. 15, pp. 2897–2904, 2007.

[68] B. Al-Duri and G. McKay, "External mass transport during dye adsorption onto carbon," in *Proceedings of the Royal Irish Academy. Section B: Biological, Geological, and Chemical Science*, vol. 90B, pp. 45–56, Royal Irish Academy, 1990.

[69] Z. A. Al-Othman, R. Ali, and M. Naushad, "Hexavalent chromium removal from aqueous medium by activated carbon prepared from peanut shell: adsorption kinetics, equilibrium and thermodynamic studies," *Chemical Engineering Journal*, vol. 184, pp. 238–247, 2012.

[70] A. C. Martins, O. Pezoti, A. L. Cazetta et al., "Removal of tetracycline by NaOH-activated carbon produced from macadamia nut shells: kinetic and equilibrium studies," *Chemical Engineering Journal*, vol. 260, pp. 291–299, 2015.

[71] A. Rahmani-Sani, A. Hosseini-Bandegharaei, S.-H. Hosseini, K. Kharghani, H. Zarei, and A. Rastegar, "Kinetic, equilibrium and thermodynamic studies on sorption of uranium and thorium from aqueous solutions by a selective impregnated resin containing carminic acid," *Journal of Hazardous Materials*, vol. 286, pp. 152–163, 2015.

[72] M. Djebbar, F. Djafri, M. Bouchekara, and A. Djafri, "Adsorption of phenol on natural clay," *Applied Water Science*, vol. 2, no. 2, pp. 77–86, 2012.

[73] T. Steiner, "The hydrogen bond in the solid state," *Angewandte Chemie International Edition*, vol. 41, no. 1, pp. 48–76, 2002.

[74] C. A. Igwegbe, J. O. Ighalo, K. K. Onyechi, and O. D. Onukwuli, "Adsorption of Congo red and malachite green using H3PO4 and NaCl-modified activated carbon from rubber (Hevea brasiliensis) seed shells," *Sustainable Water Resources Management*, vol. 7, no. 4, pp. 1–16, 2021.

[75] A. Dąbrowski, P. Podkościelny, Z. Hubicki, and M. Barczak, "Adsorption of phenolic compounds by activated carbon–a critical review," *Chemosphere*, vol. 58, no. 8, pp. 1049–1070, 2005.

[76] L. Zhang, N. Liu, L. Yang, and Q. Lin, "Sorption behavior of nano-TiO_2 for the removal of selenium ions from aqueous solution," *Journal of Hazardous Materials*, vol. 170, no. 2-3, pp. 1197–1203, 2009.

[77] J. Hu, G. Chen, and I. M. Lo, "Removal and recovery of Cr(VI) from wastewater by maghemite nanoparticles," *Water Research*, vol. 39, no. 18, pp. 4528–4536, 2005.

[78] B. Saha, S. Chakraborty, and G. Das, "A mechanistic insight into enhanced and selective phosphate adsorption on a coated carboxylated surface," *Journal of Colloid and Interface Science*, vol. 331, no. 1, pp. 21–26, 2009.